

INFLUENCE OF ACTIVE CONTROL ON STG-BASED GENERATION OF STREAMWISE VORTICES IN NEAR-WALL TURBULENCE

B.-Q. Deng, C.-X. Xu and G.-X. Cui
Department of Engineering Mechanics
Tsinghua University
Beijing, 100084, P. R. China
xucx@tsinghua.edu.cn

ABSTRACT

The near-wall streamwise vortices are closely related with the generation of high skin friction at the wall in turbulent flows, and in the controlled, friction-reduced turbulent flows, streamwise vortices are greatly attenuated. In present study, the streak transient growth (STG) mechanism of generating near-wall streamwise vortices is employed, and the opposition control is imposed during the transient growth process of the perturbation to disclose how the active control affects the generation of quasi-streamwise vortices. It is found that in the transient growth stage, when the detection plane is located near the wall ($y_d^+ = 15$), the control can suppress the generation of the streamwise vorticity through weakening the near-wall vertical velocity; when the detection plane moves away from the wall ($y_d^+ = 28$), the control has opposite effects. In the vortex generation stage, the control can not change the dominance of the stretching effect. The $y_d^+ = 15$ control can achieve sustained overall attenuation of streamwise vortex generation via the suppression of the stretching term. The $y_d^+ = 28$ control, however, generates multiple extreme points in the stretching term distribution, which causes increasing the number of streamwise vortices by splitting the primary vortex into smaller and shorter fractions. The opposition control using the signal at $y_d^+ = 28$ with reduced strength has been proposed and tested in both minimal and full-scale channel flows. The effectiveness in turbulence suppression by the lessened $y_d^+ = 28$ control confirms present analysis.

INTRODUCTION

It is widely accepted that the near-wall quasi-streamwise vortices play a dominant role in both turbulence production and high skin-friction generation (Kim, Moin & Moser, 1987). By active manipulation of these near-wall coherent structures through blowing / suction at the wall in opposite to the velocity detected at a small distance from the wall, Choi *et al.* (1994) successfully suppressed turbulence intensity as well as reduced the friction drag. It is demonstrated by the vast amount of following works (recent reviews see Collis, Joslin, Seifert & Theofilis, 2004; Kim, 2003; Kim & Bewley, 2007; Kasagi, Suzuki & Fukagata, 2009) that in the actively controlled, friction-reduced turbulent flows, the quasi-streamwise

vortices are greatly attenuated.

Although many interpretations have been proposed to the mechanism of turbulence suppression and skin friction reduction by active control from different viewpoints (see Choi, Moin & Kim, 1994; Hammond, Bewley & Moin, 1998; Farrell & Ioannou, 1996; Jimenez & Pinelli, 1999), how the control influence the generation of streamwise vortices still need further exploration. To do so, the mechanism of streamwise vortex generation in canonical wall-bounded turbulent flows need to be elucidated first.

The explanations for the generation of stream-wise vortices are categorized into two groups (Schoppa & Hussain, 2002): the so-called parent-offspring mechanism and the instability-based mechanism. Uniting the elements of parent-offspring and instability-based scenario, Schoppa & Hussain (2002) provided a more convincing mechanism - streak transient growth (STG), which is far more prevalent and energetic than normal-mode instability. In present work, the streak transient growth in a minimal channel subjected to the active opposition control is studied to disclose how the manipulations at the wall interfere with the formation and evolution of streamwise vortices, and why the difference in the detection position can have different even opposite effects on the flow. In the following, the numerical method and the STG problem formulation will be first described, and then the general response of disturbance energy and vortical structure to the control will be introduced. After that, the influence of the control on the STG-based generation process of streamwise vortices will be analyzed in details. Summary and discussion will be given at last.

PROBLEM FORMULATION

The flow of incompressible Newtonian fluid in a minimal channel subjected to active blowing/suction at the lower wall is studied by direct numerical simulation with Fourier-Chebyshev spectral method. The Reynolds number based on bulk mean velocity U_m and channel half width H is chosen to be $Re = 2800$, corresponding to the friction Reynolds number around $Re_\tau = 180$. According to Jimenez & Moin (1991), the computational domain is selected to span $\pi H \times 2H \times 0.2\pi H$ (approximately $560 \times 360 \times 110$ wall units) in streamwise (x),

wall-normal (y) and spanwise (z) directions, respectively, to get sustained turbulence as well as to isolate only one low-speed streak in the domain. Accordingly, $32 \times 129 \times 32$ grids are used.

According to Schoppa & Hussain (2002), the flow field is initialized by the single-side turbulent profile with a low-speed streak as the base flow

$$U(y, z) = U_0(y) + \frac{1}{2} \Delta u \cos(\beta z) g(y), \quad V = W = 0 \quad (1)$$

and the streamwise-dependent spanwise velocity w' as the perturbation (referred to as STG perturbation in Schoppa & Hussain (2002) and hereinafter)

$$u' = 0, \quad v' = 0, \quad w' = A \sin(\alpha x) g(y). \quad (2)$$

Here the superscript $'$ denotes the perturbations to the two-dimensional base flow $U(y, z)$.

In Eq.(1), $U_0(y)$ is composed of a laminar profile near the upper wall and a turbulent profile near the lower wall as was adopted by Schoppa & Hussain (2002). The low-speed streak is represented by $\Delta u \cos(\beta z) g(y)$, in which the spanwise wave number β is chosen to make the streak span about 100 wall units in spanwise direction, and $g(y)$ takes the form of $y \exp(-\eta y^2)$. We select η to make $g(y)$ reach maximum value at $y^+ = 20$. Once $g(y)$ is fixed, Δu is determined by the streak strength. According to Schoppa & Hussain (2002), the streak strength is quantified by the vortex line lift angle at $y^+ = 20$ as $\theta_{20} = \tan^{-1}(|\Omega_y|_{y^+=20}/|\Omega_z|_{y^+=20})$, with $\Omega_y = \partial U / \partial z$ and $\Omega_z = -dU_0/dy$.

According to Schoppa & Hussain (2002), this STG-based vortex generation scenario may be one of the dominant mechanism for near-wall streamwise vortex generation, since about 80% streaks extracted from fully developed near-wall turbulence are linearly stable. Hence in present study, the normal-mode stable streak with $\theta_{20} = 45^\circ$ is chosen and the amplitude of the the initial STG perturbation takes the value of $w'_{rms} = 0.5$. The opposition control is applied through the blowing / suction at the wall, i.e., the wall-normal velocity at a detection plane $v_{wall} = -v'_{y_d}$. In present study, two detection positions have been tested, $y_d^+ = 15$ and 28, respectively.

EVOLUTION OF THE DISTURBANCE ENERGY AND VORTICAL STRUCTURE

The time evolutions of the disturbance energy E_{3D} and its components u'^2 , v'^2 and w'^2 in no- and opposition-controlled minimal channel flow are shown in Fig.1. The vortical structures are identified and visualized by the iso-surface of $\lambda_2 < 0$. Fig.2 shows the iso-surface of $\lambda_2 = -3$ at $t^+ = 40, 65, 88, 125$ and 170 for the no-control and the two opposition control cases, respectively, to display the generation and evolution process of vortices.

According to the different characteristics in the evolution of disturbance energy and streamwise vortices, the whole process is divided into three stages: the transient growth dominated first stage ($0 < t^+ < 20$), the vortex generation dominated

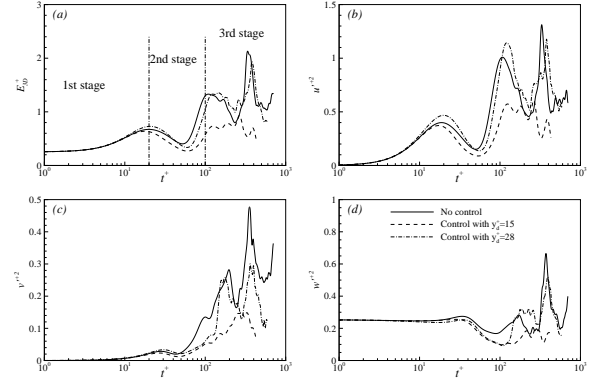


Figure 1. Time evolution of (a) E_{3D} , (b) u'^2 , (c) v'^2 and (d) w'^2 under no- and opposition- control.

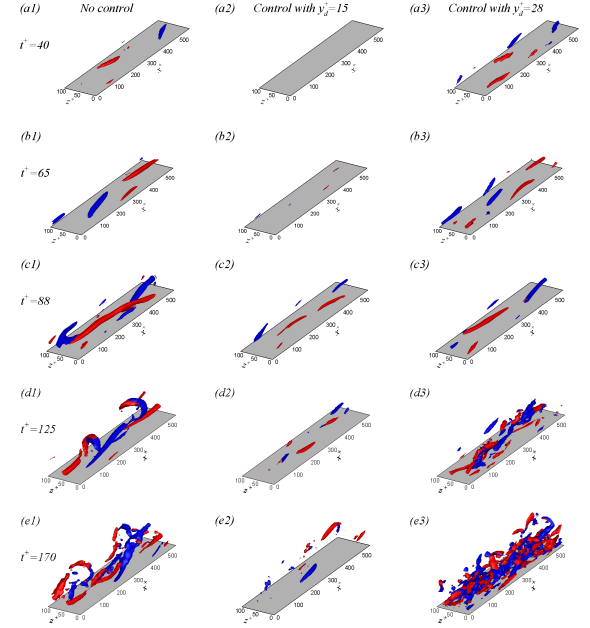


Figure 2. Iso-surface of $\lambda_2 = -3$ at $t^+ = 40$ (a1-a3), 65 (b1-b3), 88 (c1-c3), 125 (d1-d3) and 170 (e1-e3) for the cases of no-control (a1-e1), $y_d^+ = 15$ control (a2-e2) and $y_d^+ = 28$ control (a3-e3). Red: $\omega_x > 0$; Blue $\omega_x < 0$.

second stage ($20 < t^+ < 100$) and the turbulence dominated third stage ($t^+ > 100$). In the first stage, $0 < t^+ < 20$, the transient growth is the dominant mechanism, and the influence of the active control on the evolution of E_{3D} is not obvious. Initially, $u' = v' = 0$ (Eq.2). After the flow begins, u' is quickly generated, amplified and reaches a peak value at $t^+ = 20$, while the amplification of v' by the transient growth mechanism is more mild, and it reaches a far less peak value later at $t^+ = 30$. Unlike u' and v' , w' is almost unchanged and keeps the initial amplitude until the end of the first stage. The second stage covers $20 < t^+ < 100$, during which the nonlinear effects comes into to play an important role and results in the generation of quasi-streamwise vortices, as shown in Fig.2. The difference in the evolution of E_{3D} for different cases begins to appear in this stage. For the two control cases, the dis-

turbances in v' and w' are both suppressed in comparison with the no-control case. But for u' , it is attenuated by the control with $y_d^+ = 15$, but evolves in a similar way to the no-control case for the control with $y_d^+ = 28$. In this stage, the influence of the control on the generation of streamwise vortices is obvious. For the no-control case, the quasi-streamwise vortices has been formed at $t^+ = 40$, and gradually elongated in the streamwise direction (Fig.2(a1)-(c1)). Compared with the no-control case, the stream-wise vortices are greatly attenuated by the $y_d^+ = 15$ control from the very beginning of the vortex generation process (Fig.2(a2-c2)). At $t^+ = 40$, the vortices are too weak to be displayed by $\lambda_2 = -3$, hence no structures are shown in Fig.2(a2). On the other hand, by the $y_d^+ = 28$ control for $t^+ < 125$, the streamwise vortices have a similar strength to the no-control case (Fig.2(a3-c3)), but with shorter streamwise length. The third stage refers to $t^+ > 100$, after which the flow becomes turbulent. At the beginning of this stage, v' and w' undergoes abrupt growth by the control with $y_d^+ = 28$, and E_{3D} fluctuates afterwards with a magnitude similar to the no-control case. The growth in v' and w' as well as in u' under $y_d^+ = 15$ control is very limited, and E_{3D} keeps at a much lower level compared with the other two cases. In the no control case, at $t^+ = 125$ and $t^+ = 170$, as is shown by Fig.2(d1-e1), a spanwise arc is produced from the lifted downstream end of the vortices, forming a hook or hairpin vortex as was named by Robinson (1991). By the control with $y_d^+ = 15$, the vortical structures are attenuated and no hairpin vortices formed. However, at $t^+ \geq 125$, the vortices are increased in number but shortened in streamwise direction by the control with $y_d^+ = 28$, in comparison with the no-control case.

The response of the disturbance energy and streamwise vortices to the opposition control with different y_d^+ in minimal channel flow are consistent with those in full-scale channel flow (Choi, Moin & Kim, 1994). Additionally, it is worth to be addressed that the $y_d^+ = 15$ control influences the vortex generation process from the very primary stage and the vortices are attenuated all along; but the $y_d^+ = 28$ control seems only take effect after the vortices are generated and makes the number of streamwise vortices increased when the vortex tail moves away from the wall.

INFLUENCE OF THE CONTROL ON THE GENERATION OF STREAM-WISE VORTICES

How the control with different y_d^+ takes effects on the flow in the three stages will be analyzed in detail in the following.

The first stage

The first stage can be treated as a linear process since the transient growth mechanism dominates the whole period. According to Schoppa & Hussain (2002), no streamwise vortices can be generated in this stage, but the streamwise vorticity ω_x can be transiently amplified, which are necessary to trigger the stretching effect in the generation of streamwise vortices in the following nonlinear stage. Especially, since the control is imposed through the normal velocity at the wall, its effect on v' would be more straightforward and will be analyzed first. Then the influence of the control on the evolution and distribution of ω_x will be discussed.

We use the linearized Navier-Stokes equation with the continuity constraint to analyze the behavior of the flow. Recall that initially $u' = v' = 0$, and we only have w' in the form of Eq.(2) upon the base flow $U(y, z)$. Since v' and $\partial u'/\partial x$ is much smaller than w' at the beginning, $\partial u'/\partial x \sim -(\partial w'/\partial x)(\partial U/\partial z)$. And analysis shows that the variation in the spatial distribution of w' is also very small. Hence $\partial w'/\partial z$ can be neglected compared with $\partial u/\partial x$ in the continuity equation, and $\partial v'/\partial y \sim -\partial u'/\partial x \sim (\partial w'/\partial x)(\partial U/\partial z)$. Considering the form of the base flow and the STG perturbation, Eq.(1) and Eq.(2), v' should vary with x and z as $\cos(\alpha x)$ and $\sin(\beta z)$, respectively. The analysis has been confirmed by Fig.3(a1), in which the iso-surface of $|v'| = 0.01$ at $t^+ = 10$ is shown.

The variation of v' with the wall normal coordinate y is depicted by the contours of v' in the (y, z) -plane across the peak position in x direction, as is shown in Fig.3(b1-b3). One feature that should be noted is that v' changes sign in y direction around $y^+ = 20$, and reaches two extreme value around $y^+ = 9$ and $y^+ = 35$, respectively. Interestingly, if the detection plane is located at $y_d^+ = 15$, the blowing / suction velocity on the wall determined by the opposition control scheme is in opposite to v' below $y^+ = 20$. Therefore, the control with $y_d^+ = 15$ weakens v' below $y^+ = 20$ a little, as is shown in Fig.3(b2). However, when the detection plane is moved to $y_d^+ = 28$, the blowing / suction velocity on the wall is strong and its direction is the same as that of v' blow $y^+ = 20$. That means the control with $y_d^+ = 28$ can enhance v' below $y^+ = 20$. As can be seen in Fig.3(b3), v' below $y^+ = 20$ is of the same magnitude as that above $y^+ = 20$. But compared with the other two cases, v' above $y^+ = 20$ under the control is a little bit smaller.

According to Schoppa & Hussain (2002), the transient growth of the STG perturbations can lead to the formation of a sheet of streamwise vorticity ω'_x . It is first generated in the streak trough region at the streamwise position corresponding to w' 's zero-crossing point, and convected in streamwise direction by mean flow advection. With time growing, ω'_x can also be generated at the streak flank and crest, and forms a z -continuous sheet. Fig.4 shows the distribution of ω'_x in (y, z) -plane through the zero-crossing position of w' at $t^+ = 10$ and 20 for no-control and the two control cases, respectively. Though the influence of the control on ω'_x very close to the wall is obvious, the ω'_x close to the wall is less important than the elliptical patch of ω'_x in the streak trough region in the nonlinear stage. The influence of the control on the elliptical patch of ω'_x in the streak trough region is not obvious at $t^+ = 10$, but can be distinguished at $t^+ = 20$. Compared with the no-control case, ω'_x is slightly attenuated by the $y_d^+ = 15$ control, but enhanced by the $y_d^+ = 28$ control. The underlying mechanism can be explained via vorticity perturbation equations in the streak-vortex-line coordinate system (x, n, s) as is shown in Fig.5. According to Schoppa & Hussain (2002), the term $\Omega \partial u'_s / \partial x$ is dominant in the linear stage, in which u'_s is the velocity component tangential to the vortex line. If v' is negative near the left trough of the streak and positive near the right trough, just as the case shown in Fig.5, it will make favorable contribution to u'_s , vice versa. At $t^+ = 10$, the distribution of v' displays a negative region near the left trough of the streak and a positive region near the right trough of the streak for all the three cases but with different magnitude, as

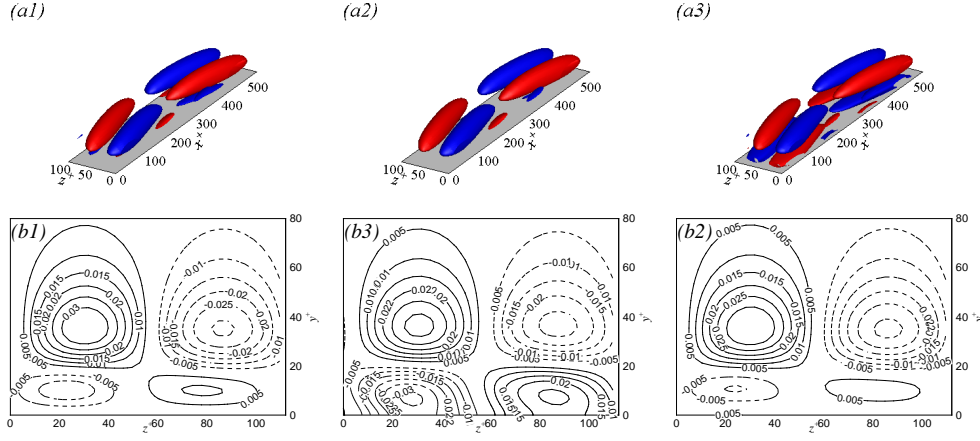


Figure 3. (a1-a3) Iso-surface of $|v'| = 0.01$ and (b1-b3) contours of v' at (y, z) -plane across the second peak position in x direction for the cases of (a1-b1) no-control, (a2-b2) $y_d^+ = 15$ control and (a3-b3) $y_d^+ = 28$ control at $t^+ = 10$. Red or solid line: $v' > 0$; Blue or dashed line: $v' < 0$.

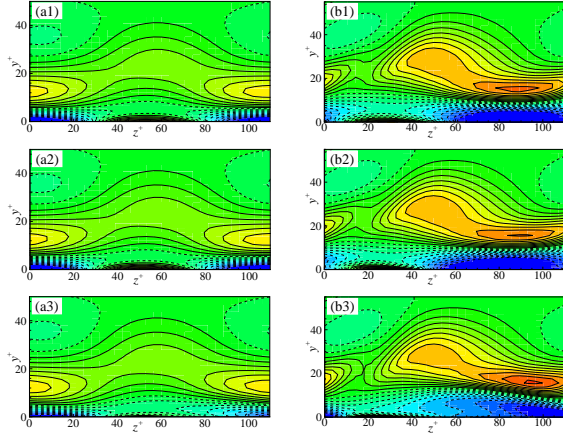


Figure 4. Contours of ω_x on (y, z) -plane at (a1-a3) $t^+ = 10$ and (b1-b3) $t^+ = 20$ for (a1-b1) no-control, (a2-b2) $y_d^+ = 15$ control and (a3-b3) $y_d^+ = 28$ control. Contour levels are from -3 to 3 in increments of 0.3. Solid lines show positive contours and dashed lines show negative contours.

has been shown in Fig.3. Because at this time, v' is still much lower than w' , the influence of the control through v' on the generation of ω_x' is negligible. At $t^+ = 20$, the $v' < 0$ region near left trough and $v' > 0$ region near right trough are suppressed by $y_d^+ = 15$ control, but greatly enhanced by $y_d^+ = 28$ control, resulting in the attenuation and magnification of ω_x' by $y_d^+ = 15$ control and $y_d^+ = 28$ control, respectively.

The second stage

After the transient growth in the first stage, the perturbations have been greatly amplified and the nonlinear effects are triggered and play an important role in the second stage, during which the streamwise vortices are generated by direct stretching the formerly produced, z -localized vorticity sheet (Schoppa & Hussain, 2002). As has been shown in Fig.2, the $y_d^+ = 15$ control can greatly attenuate the stream-wise vor-

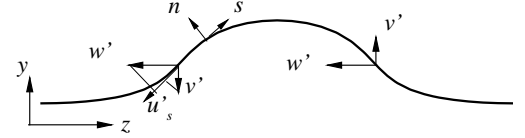


Figure 5. Schematic plot of streak-vortex-line coordinates.

trices; while the $y_d^+ = 28$ control can only affect the location and the length of stream-wise vortices. How the control influence the vortex formation in the nonlinear stage will be analyzed through the inviscid evolution equation for stream-wise vorticity ω_x :

$$\frac{\partial \omega_x}{\partial t} = -u \underbrace{\frac{\partial \omega_x}{\partial x}}_{\text{ADX}} - v \underbrace{\frac{\partial \omega_x}{\partial y}}_{\text{ADY}} - w \underbrace{\frac{\partial \omega_x}{\partial z}}_{\text{ADZ}} + \underbrace{\frac{\partial v}{\partial x} \frac{\partial u}{\partial z}}_{\text{TI1}} - \underbrace{\frac{\partial w}{\partial x} \frac{\partial u}{\partial y}}_{\text{TI2}} + \underbrace{\omega_x \frac{\partial u}{\partial x}}_{\text{ST}} \quad (3)$$

On the right-hand side of the above equation, the advection terms due to u , v and w are denoted by ADX, ADY and ADZ, respectively, TI1 and TI2 represent the contributions from tilting, and ST represent the stretching contribution.

According to Schoppa & Hussain (2002), stretching effect (ST) is the dominant factor in the generation of stream-wise vortices. In present study, the vortex with $\omega_x > 0$ at $t^+ = 40$ is studied. The vortex core, which is identified by the position of minimum λ_2 , is located at (200,17,69) for no-control, (230,20,57) for $y_d^+ = 15$ control and (230,22,65) for $y_d^+ = 28$ control cases, respectively, see Fig.2(a1-c1) for reference. In Fig.6, the vortex core is denoted by a black dot. The bold line identifies the vortex-related $\omega_x > 0$ region, and the fine lines stand for the terms concerned (solid for positive value and dashed for negative value). If ST has the same sign as ω_x at the same place, the term will make favorable

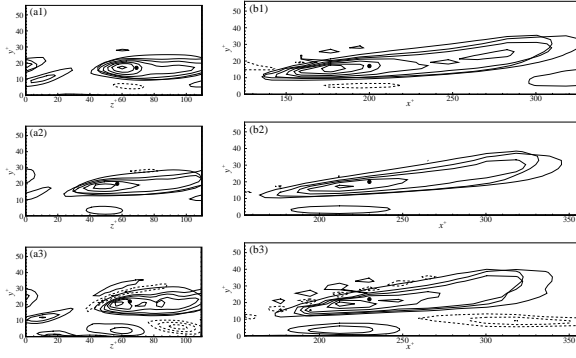


Figure 6. Contours of ST on (a1-a3) (y,z) -plane and (b1-b3) (x,y) -plane across the vortex core at $t^+ = 40$ for (a1-b1) no-control, (a2-b2) $y_d^+ = 15$ control and (a3-b3) $y_d^+ = 28$ control. Bold solid line is the iso-contour of $\omega_x = 2$ which identifies the vortex-related $\omega_x > 0$ region. The black dot shows the position of vortex core. Thin solid lines show positive ST and thin dashed lines show negative ST with contour level increments of 0.5.

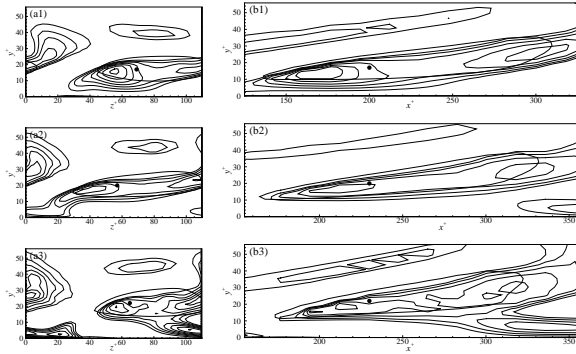


Figure 7. Contours of $\partial u/\partial x$ on (a1-a3) (y,z) -plane and (b1-b3) (x,y) -plane across the vortex core at $t^+ = 40$ for (a1-b1) no-control, (a2-b2) $y_d^+ = 15$ control and (a3-b3) $y_d^+ = 28$ control. Thin solid lines show positive $\partial u/\partial x$ with contour level increments of 0.1.

contribution to the generation of streamwise vortices. It can be seen that the distribution of ST is always in good accordance with the $\omega_x > 0$ region in both (y,z) - and (x,y) -plane for both the no-control and the two control cases, indicating that the control can not change the dominant position of ST in the formation of streamwise vortices. By the $y_d^+ = 15$ control, ST is obviously weakened, while by the $y_d^+ = 28$ control, the magnitude is not changed so much, but more local maximum regions appear within the vortex-related $\omega_x > 0$ region.

The attenuation of ST by $y_d^+ = 15$ control is easy to be understood according to the analysis of ω_x and $\partial u/\partial x$. By $y_d^+ = 15$ control, ω_x generated at the end of the first stage is smaller than that in the no-control case, while $\partial u/\partial x$ at $y^+ = 20$ has not been affected, causing the direct attenuation of ST term. The alleviated stretching term weakened the generation of streamwise vorticity, and iteratively, ω_x in the $y_d^+ = 15$ control case has not any chance to grow as much as

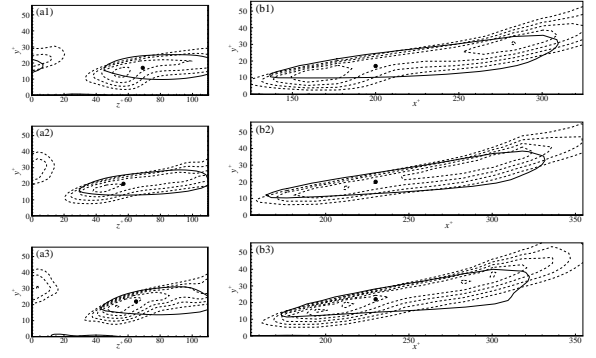


Figure 8. Contours of $\partial w/\partial x$ on (a1-a3) (y,z) -plane and (b1-b3) (x,y) -plane across the vortex core at $t^+ = 40$ for (a1-b1) no-control, (a2-b2) $y_d^+ = 15$ control and (a3-b3) $y_d^+ = 28$ control. Thin dashed lines show $\partial w/\partial x \leq -0.25$ with contour level increments of 0.1.

that in the no-control case, as is evidenced by Fig.2(a2-e2). Further analysis shows that $\partial u/\partial x$, which is directly related to ST production, is mainly generated by $-(\partial w/\partial x)(\partial u/\partial z)$ term. For $y_d^+ = 15$ control, both $-\partial w/\partial x$ (Fig.8) and $\partial u/\partial z$ are attenuated. For $y_d^+ = 28$ control, no suppression can be observed in both $-\partial w/\partial x$ and $\partial u/\partial z$, but it has been clearly elucidated that the more extreme points in ST is originated from $-\partial w/\partial x$.

It is also interesting to note that when the vortex is generated around $y^+ = 20$, the vertical velocity sensed at $y_d^+ = 15$ and $y_d^+ = 28$ is in the same phase, but with different magnitude. Their different influence on ST, and finally on streamwise vortices suggests that the strength of wall blowing / suction is crucial to the control, not only the detection position. This will be further discussed in the final section.

The third stage

In the third stage, the flow in no control and $y_d^+ = 28$ control cases becomes turbulent, while it tends to be laminar by $y_d^+ = 15$ control. As has been shown in Fig.2, the streamwise vortices under $y_d^+ = 28$ control are similar to no control case before $t^+ = 125$, but are broken into smaller and shorter fractions afterwards. We first resorted the explanation to the stretching term ST. As is discussed in the previous section, multiple extreme points in ST can be found within the primary elongated vortices. This means that the stretching strength is not uniform in the primary vortex, which can be broken into many fractions under scattered strong stretching effect. It should be addressed that the multiple extreme points in ST originating from $\partial w/\partial x$, as is elucidated in the previous section, is the result of the interaction between the flow injected on the wall and the primary vortices.

SUMMARY AND DISCUSSION

The effect of the opposition control on the STG-based generation of the near-wall streamwise vortices is studied by the direct numerical simulation of the minimal channel flow at $Re_\tau = 180$. The normal mode stable streak with $\theta_{20} = 45^\circ$ is considered. The initially imposed STG perturbation is set to

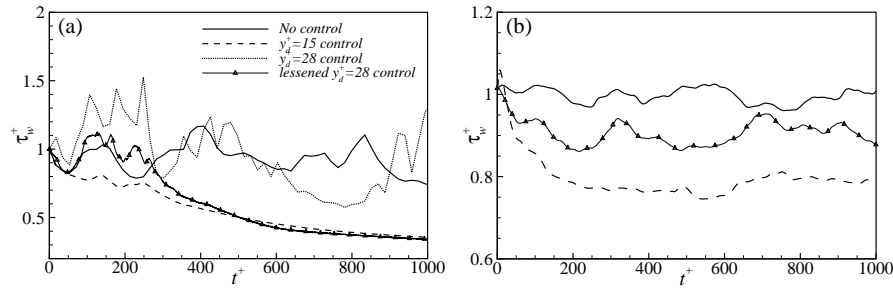


Figure 9. Time history of the plane-averaged wall shear stress. (a) minimal channel; (b) full-scale channel.

reach maximum value at $y^+ = 20$. It is found that in the linear transient growth period, v' changes sign around $y^+ = 20$, and hence $y_d^+ = 15$ control can weaken v' below $y^+ = 20$, while $y_d^+ = 28$ control can strengthen v' there, resulting in the suppression and enhancement of the streamwise vorticity generated in the z -localized elliptical patch of streamwise vorticity sheet, respectively. In the nonlinear vortex generation stage, it is found that the stretching effect is still dominant over advection and tilting effects, no matter whether the control is imposed or not. By $y_d^+ = 15$ control, the alleviated streamwise vorticity production in the linear stage takes effect directly to the suppression of the stretching term, and iteratively causing the sustained overall attenuation of streamwise vortex generation. By $y_d^+ = 28$ control, however, the stretching term keeps similar strength as that in no-control case, but with more extreme points originating from the interaction between the strong wall blowing / suction and the streak meandering. The streamwise vortices generated under $y_d^+ = 28$ control are similar to those in no-control case in early time, but are split into smaller and shorter fractions in later time due to the multiple extreme regions in stretching term distribution within the primary elongated streamwise vortices.

Although the vertical velocity imposed at the wall by $y_d^+ = 28$ control is opposite in sign to that by $y_d^+ = 15$ control in the linear stage, after the vortices are generated, the wall blowing/suction determined by the signals sensed at $y_d^+ = 15$ and 28 are in the same phase but with different strength. It is reasonable to suppose that the opposition control using the signal at $y_d^+ = 28$ but with a reduced strength can also suppress turbulence through the attenuation of the already-existing streamwise vortices. To test this conjecture, we performed the simulations to the minimal channel flow with $v_{wall} = -0.5v_{y_d^+=28}$. It is found that the lessened opposition control with $y_d^+ = 28$ can not effectively suppress the generation of streamwise vortices in the first and second stage just as $y_d^+ = 15$ control does, as can be expected, but exhibits its effects in turbulence stage. We use the time history of the plane-averaged wall skin friction to signify the turbulence levels in the channel, see Fig.9(a). For the lessened $y_d^+ = 28$ control, it follows the curves of no-control and $y_d^+ = 15$ control when $t^+ < 60$, and then grows slightly higher than the no-control case until $t^+ = 260$. After that it differs from the no-control case, and evolves towards the $y_d^+ = 15$ control case, and hence our conjecture is confirmed. That is because the lessened opposition control with $y_d^+ = 28$ can only take effect to the already-existing streamwise vortices, while the $y_d^+ = 15$ control can interfere in the generation process of the vortices.

We also tested the lessened $y_d^+ = 28$ control in the full-scale turbulent channel flow at $Re_\tau = 180$, and compared with the $y_d^+ = 15$ control, see Fig.9(b) for the time evolution of wall skin friction. It can be seen that in the full-scale turbulent channel flow, the lessened $y_d^+ = 28$ control is still effective, as is supposed to, and the skin friction is reduced by about 10%, in comparison with the 22% reduction in skin friction achieved by $y_d^+ = 15$ control.

ACKNOWLEDGEMENT

The work is supported by National Science Foundation of China (Grant No. 10925210).

REFERENCES

- Choi, H., Moin, P. & Kim, J. 1994 Active turbulence control for drag reduction in wall-bounded flows. *J. Fluid Mech.* **262**, 75–110.
- Collis, S. S., Joslin, R. D., Seifert, A. & Theofilis, V. 2004 Issues in active flow control: theory, control, simulation, and experiment. *Prog. Aero. Sci.* **40**, 237C289.
- Farrell, B.F. & Ioannou, P. 1996 Turbulence suppression by active control. *Phys. Fluids* **8**, 1257–1268.
- Hammond, E.P., Bewley, T.R. & Moin, P. 1998 Observed mechanisms for turbulence attenuation and enhancement in opposition-controlled wall-bounded flows. *Phys. Fluids* **10**, 2421–2423.
- Jimenez, J. & Pinelli, A. 1999 The autonomous cycle of near-wall turbulence. *J. Fluid Mech.* **389**, 335–359.
- Jimenez, J. & Moin, P. 1991 The minimal flow unit in near-wall turbulence. *J. Fluid Mech.* **225**, 213–240.
- Kasagi, N., Suzuki, Y. & Fukagata, K. 2009 Microelectromechanical systems-based feedback control of turbulence for skin friction reduction. *Annu. Rev. Fluid Mech.* **41**, 231–251.
- Kim, J. 2003 Control of turbulent boundary layers. *Phys. Fluids* **15**, 1093–1105.
- Kim, J. & Bewley, T. R. 2007 A linear systems approach to flow control. *Annu. Rev. Fluid Mech.* **39**, 383–417.
- Kim, J., Moin, P. & Moser, R. D. 1987 Turbulence statistics in fully developed channel flow at low Reynolds number. *J. Fluid Mech.* **177**, 133.
- Robinson, S. K. 1991 Coherent motions in the turbulent boundary layer. *Annu. Rev. Fluid Mech.* **23**, 601–639.
- Schoppa, W. & Hussain, F. 2002 Coherent structure generation in near-wall turbulence. *J. Fluid Mech.* **453**, 57–108.